Received: 14 October 2024 | Accepted: 9 September 2025

DOI: 10.1111/syen.70011

ORIGINAL ARTICLE

Systematic Entomology | Royal Entomological Society

How many cows are in the desert? Molecular phylogeny and species delimitation of the genus *Gyriosomus* (Coleoptera: Tenebrionidae: Pimeliinae) from the Atacama Desert

Simón Anguita-Salinas[1,2] | Marcelo Guerrero[2] | Víctor M. Diéguez[2] | Pablo Pinto[3] | Sebastián Larrea-Meza[3] | Alfonso Jara-Flores[4] | Reinhard Predel[4] | Álvaro Zúñiga-Reinoso[2,4]

[1]Programa de Doctorado en Sistemática y Biodiversidad, Universidad de Concepción, Concepción, Chile

[2]Grupo de Estudios en Coleóptera del Cono Sur (GrECCo-Sur), Santiago, Chile

[3]Escuela de Ciencias Agrícolas y Veterinarias, Universidad Viña del Mar, Viña del Mar, Chile

[4]Institut für Zoologie, Universität zu Köln, Köln, Germany

Correspondence
Álvaro Zúñiga-Reinoso, Institut für Zoologie, Universität zu Köln, Köln, Germany.
Email: azunigar@uni-koeln.de

Funding information
Deutsche Forschungsgemeinschaft

Editor: Gael J. Kergoat

Abstract

Gyriosomus is a genus of charismatic tenebrionids endemic to Chile, commonly known as *vaquitas del desierto*'. They are distributed from ~25° S to ~34° S, almost exclusively within the Coquimban Biogeographic Province. They are notable for the explosive and massive appearance of adults associated with blooming desert events in Atacama. Since their initial description in 1834, 44 species have been classified, but the genus has not undergone a comprehensive systematic revision. Using molecular markers, taxonomic issues related to the use of morphological characters have recently been identified. In this study, we evaluated the phylogenetic relationships within *Gyriosomus* and the congruence of the current taxonomic scenario with our results. We conducted an exhaustive sampling across the entire distribution range of the genus. Specifically, we reconstructed a molecular phylogeny based on four genes (cytochrome *c* oxidase subunit I 'COI', wingless 'Wg', carbamoyl phosphate synthetase 'CAD' and 28S ribosomal RNA '28S') with 41 of the 44 described species and performed unilocus and multilocus molecular species delimitation analyses. The phylogenetic analyses indicate that the 45 genetically evaluated species are organized into nine distinct clades. Only half of the previously described species were validated by the molecular species delimitation analyses. The rest are likely new candidate species, with some potentially being synonyms. External morphology alone may not be sufficient to support the taxonomy due to the plasticity of these characters. We also found a zone of 'High Cladistic Sympatry', inhabited by representatives of different clades. In this zone, we encountered polymorphic and cryptic species and a high degree of convergence between clades, which complicates the study of these darkling beetles.

KEYWORDS
blooming desert, cline, El Niño/La Niña phenomena, Nycteliini, *vaquitas del desierto*

INTRODUCTION

The genus *Gyriosomus* Guérin-Méneville is a genus of darkling beetles (Tenebrionidae) from the subfamily Pimeliinae Latreille, which comprises 44 described species endemic to north-central Chile (Guerrero et al., 2023). They belong to the South American tribe Nycteliini Solier and are one of the most diverse genera of this tribe (Flores, 1997). Within Nycteliini, *Pilobalia* Burmeister was inferred as

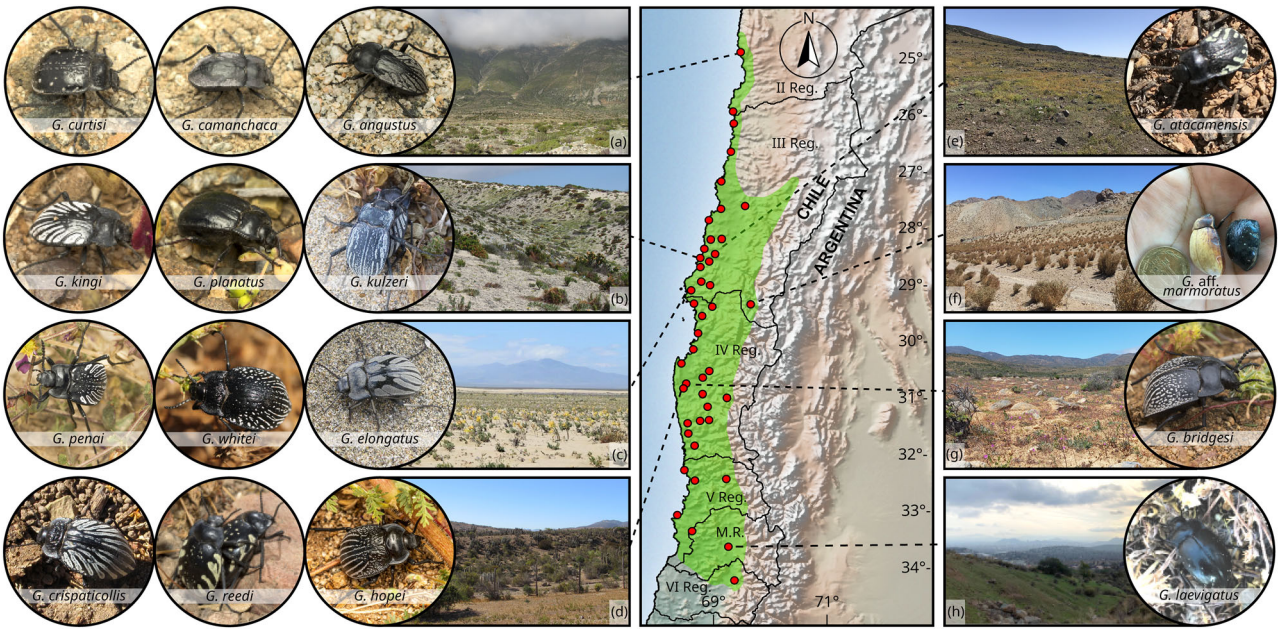

FIGURE 1 Overview of the distribution and collection sites of *Gyriosomus* analysed in this study. (a) Alluvial terraces of Paposo, habitat of *G. curtisi*, *G. camanchaca* and *G. angustus*; (b) Guacolda dunes, habitat of *G. kingi*, *G. planatus* and *G. kulzeri*; (c) Punta de Choros dunes, habitat of *G. penai*, *G. whitei* and *G. elongatus*; (d) Socos hills, habitat of *G. crispaticollis*, *G. reedi* and *G. hopei* respectively; (e) habitat of *G. atacamensis* on the slopes of Freirina Hill; (f) habitat of *G.* aff. *marmoratus* in the high-altitude thorny scrub of the Elqui Cordillera; (g) habitat of *G. bridgesi* in the hills of Talinay; (h) hill slope next to Santiago, typical habitat of *G. laevigatus*.

the sister genus of *Gyriosomus* in the phylogenomic study of Ragionieri et al. (2023), which included only six out of 12 genera of Nycteliini (Bouchard et al., 2021). These charismatic insects are commonly known in Chile as '*vaquitas del desierto*' ('little cows of the desert') due to their black colouration with white spots on the elytra (Peña, 1959). The distribution of this genus ranges from the coast of Paposo in the north (~25° S) to the foothills of Machalí in the south (~34° S) (Pizarro-Araya & Jeréz, 2004, Figure 1). In the north, the distribution of *Gyriosomus* is restricted to a narrow coastal strip from 28° S up to 25° S, where only three species reach this distributional limit (Zúñiga-Reinoso et al., 2019). However, approximately 90% of *Gyriosomus* species are concentrated in the coastal terraces and interior plains of the Coquimbo and Atacama political regions within the Coquimban Biogeographic Province (CBP), exhibiting a high degree of endemism (Pizarro-Araya & Flores, 2004).

Adults are diurnal and epigean, frenetically roaming the desert in search of food and mates for copulation (Peña, 1959; see also Figure 2). They are considered phytophagous-polyphagous insects, as they have been observed consuming flowers, stems and leaves of xeric plants. However, they have also been reported preying on lepidopteran larvae and feeding on vertebrate carrion (Pizarro-Araya, 2010), as well as on the corpses of other insects and even on dead individuals of their own species (Mondaca, 2004). On the other hand, the larvae are hypogean, presumed to be phytophagous and could be found below the soil (Mondaca, 2004). Both larvae and adults contribute to the decomposition of organic matter by consuming detritus, thereby influencing the availability of nutrients for primary productivity in the desert (Pizarro-Araya, 2010). Additionally, they are consumed by other invertebrates and vertebrates, playing multiple roles in the food web (Peña, 1959; Pizarro-Araya, 2010; Vidal et al., 2011).

Roig-Juñent and Flores (2001) indicate that the genus is one of the endemic elements of the coastal Atacama Desert, with an ancient xeric origin suggested by its adaptations to these extreme environments. One of the most remarkable adaptations of this group is their sudden mass appearance just after rare rainfall events in the Atacama Desert. This phenomenon is mostly associated with late winter rainfalls in the desert exceeding 20 mm, generating a spectacular but irregular event known as the blooming desert (Chávez et al., 2019; Vidiella et al., 1999). This ecological event is mostly associated with the El Niño climate phenomenon with precipitation driven by the rise of Pacific Ocean's temperatures, the opposite scenario is known as the La Niña climate phenomenon (ENSO, Arntz & Fahrbach, 1996). Diapause in *Gyriosomus* could allow them to persist for several consecutive years without rain (Cepeda-Pizarro et al., 2005b). However, it is still unknown at which life stage they persist through extended dry periods, although pupae diapause seems very likely (Cepeda-Pizarro et al., 2005b). This strategy of mass adults' appearance, related to annual plant growth after rainfall, has also been reported for other desert-adapted tenebrionids, such as the Namibian *Pachynotelus* Solier (Pimeliinae: Cryptochilini), which, like *Gyriosomus* exhibits daylight activity and a white dots/stripes colouration pattern (Seely & Louw, 1980).

The highly irregular population dynamics make it challenging to study *Gyriosomus*, and to date, there is no comprehensive and up-to-date taxonomic or systematic revision for the genus. Most existing

FIGURE 2 Field observations of behaviour of *Gyriosomus*. (a) Congregation of *G.* aff. *paulseni* individuals on dry grass; (b) *G. confusus* sheltering in the sand; (c) *G. melcheri* individuals recently exposed from their refuge under a stone, showing the variation in elytral design within a population; (d) courtship of a *G. leechi* male on a female while she feeds on Cyperaceae leaves; (e) *G. chango* feeding on plant detritus; (f) *G. planicollis* female feeding on freshly fallen petals; (g) *G. angustus* female climbing on *Solanum* sp. (Solanaceae) to forage on fresh foliage; (h) *G. hopei* individuals feeding on the carcasses of a conspecific that was run over moments earlier by a car; (i) congregation of *G. elongatus* males at sunset searching for females; (j) interspecific copulation between *G. whitei* (♂) and *G. confusus* (♀); (k) interspecific copulation between *G. kingi* (♂) and *G. kulzeri* (♀); (l) interspecific courtship of *G. camanchaca* (♂) and *G. curtisi* (♀).

studies focused on the description of new species (e.g., Mondaca, 2004; Pizarro-Araya & Flores, 2004; Guerrero & Vidal, 2018; Zúñiga-Reinoso et al., 2019; Guerrero & Aceituno, 2020). The early species descriptions are usually brief and imprecise (see Guerrero et al., 2023; Pizarro-Araya & Flores, 2006), and the loss of type material or the unavailability of them (e.g., not having been returned) in some museum collections further complicates a taxonomic revision of this genus. The first species were described under the genus *Nyctelia*: *N. hopei* Gray and *N. luczotii* Guérin-Méneville. Later, Guérin-Méneville (1834) established the genus *Gyriosomus* to include these two species along with four new species (*G. curvilineatus* Guérin-Méneville—a synonym of *G. luczotii*—*G. impressus* Guérin-Méneville, *G. laevigatus* Guérin-Méneville and *G. lineatus* Guérin-Méneville; the latter now classified under *Geoborus* Blanchard). Gebien (1937) designated *G. luczotii* as the type species for the genus. Subsequently, some species were synonymized (see Gebien, 1937, 1944; Peña, 1966b), the subspecies were elevated to species status (e.g., Guerrero & Aceituno, 2020) and others were revalidated (e.g., Guerrero et al., 2023). By the second half of the 20th century, 34 species had been described (Pizarro-Araya & Jeréz, 2004). Over

the past two decades, there has been a prolific process of describing new species, bringing the total to 44 described species today (see Guerrero & Aceituno, 2020; Guerrero & Vidal, 2018; Mondaca, 2004; Pizarro-Araya & Flores, 2004; Zúñiga-Reinoso et al., 2019).

Traditionally, species descriptions relied solely on external morphological evidence, such as pronotal and elytral shape and design. Only recently genital morphology and COI data (widely used for molecular barcoding) have been incorporated into the study of *Gyriosomus* (see Guerrero et al., 2023; Zúñiga-Reinoso et al., 2019). Barcoding data has allowed for the detection of a putative new species and the revalidation of another, indicating the presence of cryptic species within this group (see Guerrero et al., 2023; Zúñiga-Reinoso et al., 2019). Additionally, a high degree of intraspecific/intersexual polymorphism in pronotal and elytral design was detected (Guerrero et al., 2023). Therefore, based on recent evidence, it is likely that taxonomy relying solely on external morphology does not accurately reflect the true diversity of *Gyriosomus*. In this study, we conducted a comprehensive biological and systematic review of the genus *Gyriosomus* benefitting from more than 20 years of field observations and inferred a molecular phylogeny which is based on one mitochondrial and three nuclear gene fragments. Additionally, we assessed the group's diversity through a series of unilocus and multilocus molecular species delimitation analyses.

MATERIALS AND METHODS

Sampling

Specimens were collected throughout the known distribution of *Gyriosomus*, from Paposo (24.5° S, 70.5° W) to Machalí (34.2° S, 70.6° W) and from sea level to 3100 m. asl. (see Table S1). Collections were conducted from 1997 to 2024 in the months of September, October and November. Specimens for DNA analysis were collected in 2011, 2015, 2017, 2020, 2021, 2022, 2023 and 2024. These specimens were opened, separating the head from the pronotum, and preserving the whole specimen in 96% ethanol for subsequent laboratory analysis. Authorizations were obtained to conduct sampling in Protected Wild Areas of the State of Chile (permits No. 005/2017, 105/2020, 016/2021 and 039/2023). A total of 41 out of the 44 described species of the genus were sampled; only *G. granocostatus* Fairmaire, *G. impressus* and *G. lucens* Kulzer were not collected. For the identification of the material, bibliographic resources were used (e.g., Guerrero & Aceituno, 2020; Guerrero et al., 2023; Guerrero & Vidal, 2018; Mondaca, 2004; Pizarro-Araya & Flores, 2004; Zúñiga-Reinoso et al., 2019). Additionally, type material from various museums was reviewed, including the National Museum of Natural History in Santiago (Chile), the Naturhistorisches Museum Basel in Basel (Switzerland), the Muséum national d'Histoire Naturelle in Paris (France) and the Museum of Zoology at the University of Concepción in Concepción (Chile). Material from personal collections was also examined (those of Víctor M. Diéguez, Marcelo Guerrero, Pablo Pinto, Sebastian Larrea and the Luis Peña collection of Pedro Vidal). Additionally, species described in Zúñiga-Reinoso et al. (2019) and Guerrero et al. (2023) were included, from which we obtained a complementary set of gene fragments (i.e., CAD, Wg and 28S).

DNA extraction, amplification and sequencing

DNA was extracted from thoracic muscle tissue using the EZNA Insect DNA kit (Omega Bio-tek, Inc., Norcross, U.S.A.). Almost complete mitochondrial COI was first amplified for 153 specimens (Table S1). To detect diversity in more conserved markers, genetic distances for COI were calculated for major *Gyriosomus* clades: For groups that showed a genetic distance ≥2%, a specimen was subsequently selected to amplify more conserved complementary genes, such as the nuclear genes CAD and Wg (see Table S1). However, for the highly conserved nuclear 28S, only one individual per group exhibiting a genetic distance greater than 10% was selected (see also Tables S1 and S2 for the list of primers). The thermal polymerase chain reaction (PCR) steps were 94°C for 2 min, followed by 36 cycles at 94°C for 30 s, 53–56°C for 45 s and 72°C for 1 min, with a final extension at 72°C for 2 min. Each reaction included 5 μL of MgCl2, 2 μL of dNTPs (10 nM), 0.5 μL of each primer (100 nM), 1.5 U Taq polymerase (Biozym) and 50–100 ng of template DNA, in a final volume of 48 μL. The PCR products were purified using the peqGOLD Cycle-Pure kit (Peqlab Biotechnologie GmbH, Erlangen, Germany) and sequenced in both forward and reverse directions at Eurofins Genomics GmbH (Germany) using the Sanger sequencing method. The sequences from each sample were reviewed and edited using the program BIOEDIT v.7.0.5.3 (Hall, 1999). A matrix for each gene was created by aligning the sequences using the ClustalW algorithm (Thompson et al., 1994) within BIOEDIT v.7.0.5.3. The matrices were manually reviewed to discard any inconsistencies. The Xia test (Xia et al., 2003) implemented in DAMBE v.5.1.5 (Xia & Xie, 2001) was performed to evaluate the saturation of each gene matrix (see Table S3).

Phylogenetic reconstruction

The phylogenetic reconstruction was performed by concatenating the COI, Wg, CAD and 28S genes using Bayesian Inference (BI) and maximum likelihood (ML) algorithms. First, for both phylogenetic reconstruction, the codon partitioning within each coding gene was assessed using Partition Finder v.2.1.1 (Lanfear et al., 2017), and the best models for sequence evolution for all phylogenetic analyses were selected based on the Akaike Information Criterion (AIC) using ModelFinder (Chernomor et al., 2016; Kalyaanamoorthy et al., 2017) implemented in the IQ-TREE web server (Trifinopoulos et al., 2016; see models in Table S3). The Bayesian phylogeny was reconstructed using MrBayes v.3.2 (Ronquist et al., 2012) with all concatenated genes, employing the Markov Chain Monte Carlo (MCMC) method. Four independent analyses were run for 10 million generations, sampling every 1000 generations, using four Markov chains (one cold and three

heated) with a temperature parameter set to 0.20 and discarding the first 25% as burn-in. To confirm the convergence of the MCMC runs, we check the potential scale reduction factor (PSRF, value = 1.0 for runs convergence) for TL, Kappa and Alpha parameters, which the optimum sampling was checked with the estimated sample size (ESS, value >100 for adequate parameters sampling, see Table S4). The ML phylogeny was reconstructed using IQ-TREE v1.6 (Nguyen et al., 2015) implemented in the IQ-TREE web server (Trifinopoulos et al., 2016). Perturbation strength of 0.5 and 100 IQ-TREE stopping rule were previously set. Branch support was obtained using ultrafast bootstrap (Hoang et al., 2018) with 1000 bootstrap alignments, 1000 maximum iterations and 0.99 minimum correlation coefficient; and Shimodaira–Hasegawa approximate likelihood ratio test (Guindon et al., 2010) with 1000 replicates. The phylogenies were rooted with the Praociini *Antofagapraocis brevipilis* Flores, as member of sister tribe of Nycteliini (Ragionieri et al., 2023). The Nycteliini *Entomoderes erebi* (Lacordaire) and *Pilobalia decorata* (Erichson), genera closely related to *Gyriosomus* (Flores, 2000; Ragionieri et al., 2023), were also included. The resulting trees were visualized and edited using the FigTree v.1.2.2 software (Rambaut, 2009).

For the following molecular species delimitation analyses, trees based on the COI gene fragment had to be constructed. Firstly, for the Poisson tree process (PTP) analyses, an ML tree and a Bayesian tree were constructed in IQ-TREE (Nguyen et al., 2015) and MrBayes v.3.2 (Ronquist et al., 2012), respectively, using the COI gen matrix. The codon partitions and substitution models used and all trees were reconstructed as previously described. Secondly, for GMYC analyses, an ultrametric Bayesian tree was constructed in BEAST v1.8 (Drummond & Rambaut, 2007), the substitution models selected by ModelFinder were replaced by GTR + I + G; meanwhile, the Birth-Death speciation model was selected over the Yule speciation model according to Model Comparison with AIC through MCMC analysis (AICM) performed in Tracer v1.6 (Drummond & Rambaut, 2007) (see Table S4). The reconstruction ran for 50 million generations sampling every 5000 generations, burning the first 20% of the generations. Results were checked with Tracer v1.6 (Drummond & Rambaut, 2007) to confirm the chain convergence, with all parameters with ESS values above 200. The sampled trees were combined in TreeAnnotator v1.8.0 (Drummond & Rambaut, 2007).

All files for each reconstruction are available in https://www.crc1211db.uni-koeln.de/search/view.php?dataID=1034.

Molecular species delimitation

To proceed with the unilocus molecular species delimitation analyses, we created a matrix using the mitochondrial COI gene fragment and we calculated *p*-distance in Mega X (Kumar et al., 2018). This marker was chosen for its high variability among the gene set in this study and its widespread use as a barcode gene in insects (e.g., DeWaard et al., 2019; Virgilio et al., 2010). Then, we ran four methodologies for unilocus and one multilocus species delimitation.

First, we analysed the data using PTP approaches: standard PTP (sPTP) and Bayesian PTP (bPTP). PTP is a tree-based approach that can determine the transition between processes occurring among species and within a species using a two-parameter model (speciation and coalescence). The fit between these parameters delimits species based on the topology (Zhang et al., 2013). For these analyses, the COI trees reconstructed with MrBayes v.3.2 and IQ-TREE were used. The sPTP analysis was conducted on the mPTP webserver (https://mptp.h-its.org/) with a 0.95 percentile cutoff. While bPTP analysis was performed on the PTP webserver (https://species.h-its.org/ptp), sampling 500,000 generations and discarding the first 10% as burn-in. Secondly, we used the software Generalized Mixed Yule Coalescent (GMYC), which is also a tree-based approach that fits within and between species branching models from gene trees (Fujisawa & Barraclough, 2013). For this analysis, the COI ultrametric tree reconstructed with BEAST v1.8 was used. The GMYC analysis was performed on the GMYC web server (https://species.h-its.org/gmyc/) considering a single threshold. Then, we analysed the data with the software Automatic Barcode Gap Discovery (ABGD), a distance-based algorithm that separates candidate species based on the barcoding gap (a gap in the distribution of pairwise genetic distances) expected between interspecific and intraspecific distances (Puillandre et al., 2012). The recursive version of ABGD (ABGDr) was conducted using the ABGD web server (https://bioinfo.mnhn.fr/abi/public/abgd/abgdweb.html). The analysis considered simple genetic distances and interspecific divergence priors between 0.001 and 0.25, with 100 steps and applying a relative gap width of 1. Also, we used the software Assemble Species by Automatic Partitioning (ASAP), another distance-based algorithm that ranks the species partitioning with scores that use no biological prior insight of intraspecific diversity (Puillandre et al., 2021). ASAP was conducted on the ASAP web server (https://bioinfo.mnhn.fr/abi/public/asap/). The analysis was executed with settings by default, considering a simple genetic distance.

Finally, we validate our species delimitation proposal with the package Species Tree And Classification Estimation, Yarely (STACEY), that simultaneously infers species trees and species delimitations under multispecies coalescent model with multilocus datasets (Jones, 2017). To perform STACEY v1.3.1, the whole dataset with COI, 28S, CAD and Wg genes was used. We compared two consensus scenarios based on the results of the unilocus analyses: one with the minimum number of species according to those analyses (from now 'lumping' scenario); the other, a majority consensus that recovers the candidate species supported by most of the unilocus analyses (from now 'splitter' scenario). The analyses were performed with BEAST2 v2.7.7 (Bouckaert et al., 2019) with default substitution models and strict clock model with default rates for each gene. The MCMC runs were performed for 500 million generations sampling every 50,000 generations, burning the first 20% of generations. Run convergence was checked with Tracer v1.6 (Drummond & Rambaut, 2007). Candidate species were delimited from the tree file using the package SpeciesDelimitationAnalyser (speciesDA.jar) (burning 20%, -collapseheight = 0.00001 and -simcutoff = 1.0). The species delimitation scenario was selected according to the best count fraction value (i.e., >75%).

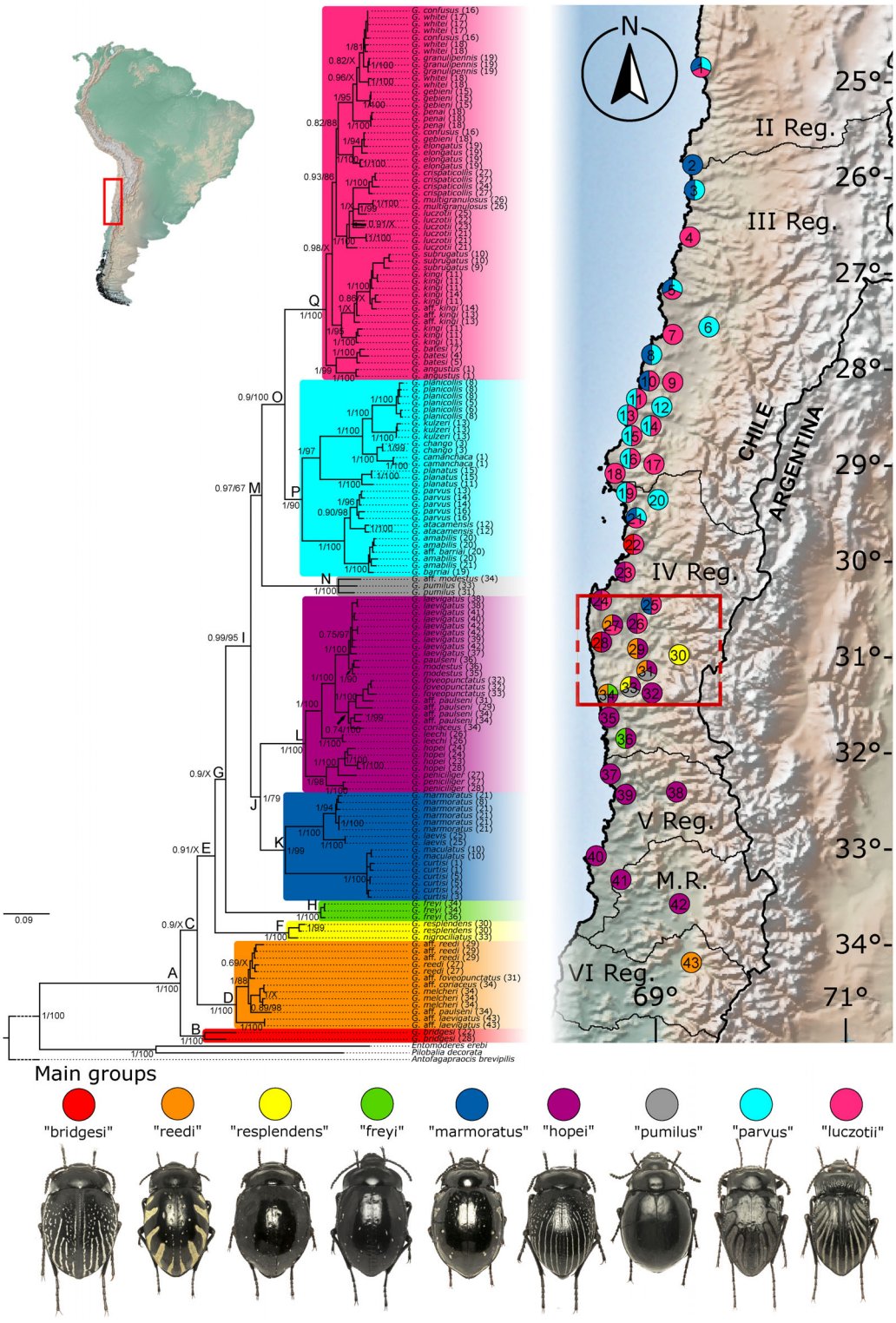

FIGURE 3 Bayesian phylogenetic tree for the genus *Gyriosomus*, derived from concatenated COI, 28S, CAD and Wg genes, showing branches in common with the maximum likelihood reconstruction. The coloured boxes indicate the nine main clades/groups identified, characteristic morphologies for each clade/groups shown below the tree. Posterior probability (PP) and ultrafast bootstrap (UFB) values are displayed near each node, while discrepancies with maximum likelihood reconstruction are indicated with 'X'. To the right of the tree, a distribution map of each clade (colour-coded as in the tree) is provided based on the sampled localities. The red box highlights the Zone of High Cladistic Sympatry (ZHCS).

RESULTS

Phylogenetic reconstruction

A concatenated matrix of 3687 base pairs was obtained in total (available at CRC1211 Database, https://www.crc1211db.uni-koeln.de/search/view.php?dataID=1034), with 697 parsimony-informative sites. None of the genes used exhibited signs of saturation. Additionally, heterozygous sites were found in the nuclear genes Wg and CAD (further information in Table S3).

The Bayesian phylogenetic reconstruction obtained from the concatenated four-gene dataset reveals a consistent phylogeny, with almost all nodes having high support values (posterior probability [PP] ≥ 0.95, except for branches C, E, G and O). The ML phylogenetic reconstruction suggested a different topology with some branches with suboptimal support values (ultrafast bootstrap value [UFB] < 95%, Shimodaira–Hasegawa approximate likelihood ratio test [SH-aLRT] < 80%) (see Figure S1; tree files are available at https://www.crc1211db.uni-koeln.de/search/view.php?dataID=1034). To describe the phylogenetic reconstructions, the BI topology is shown, indicating also the branches in common with the ML reconstruction given the UFB values, and for describing our results, basing our identification according to the current taxonomical arrangement: *Gyriosomus* is recovered as a monophyletic group (node A, PP = 1, UFB = 100%, SH-aLRT = 100%), sister to *Entomoderes* Solier and *Pilobalia* Burmeister. Within *Gyriosomus*, we identified nine well-supported major clades/groups (nodes/branches B, D, F, H, K, L, N, P and Q) (Figure 3).

The first lineage to diverge from the rest is *G. bridgesi* Waterhouse (clade B, PP = 1, UFB = 100%, SH-aLRT = 100%). Next, the clade C as sister to clade B (PP = 0.9) is divided in the 'reedi group' (clade D, PP = 1, UFB = 99.9%, SH-aLRT = 100%) and clade E (PP = 0.91). The 'reedi group' is subdivided into the *G.* aff. *laevigatus* specimens from Machalí (see Figure 3, loc. 43) as sister to the rest of that group (PP = 1, UFB = 100%, SH-aLRT = 100%), which further splits into two subclades (PP = 1, UFB = 88%, SH-aLRT = 89.6%). One subclade includes the *G.* aff. *paulseni* from Canela (see Figure 3, loc. 34) as sister to *G. coriaceus* Fairmaire from northern Huentelauquen (see Figure 3, loc. 34) + *G. melcheri* Kulzer (PP = 0.89, UFB = 98%, SH-aLRT = 87.8%), while the other subclade contains *G.* aff. *foveopunctatus* Fairmaire from Soruco (see Figure 3, loc. 31) + *G. reedi* Kulzer + *G.* aff. *reedi* (PP = 0.69). The clade E has the 'resplendens group' (clade F, PP = 1, UFB = 100%, SH-aLRT = 100%) as sister to the rest of the lineages (clade G, PP = 0.9). The 'resplendens group' contains *G. resplendens* Aceituno & Guerrero as sister to *G. nigrociliatus* Guerrero & Aceituno.

Within the clade G, *G. freyi* Gebien (clade H, PP = 1, UFB = 100%, SH-aLRT = 99.9%) diverges from the remaining species (clade I, PP = 0.99, UFB = 95%, SH-aLRT = 99.6%). Next, within clade I, clades J (PP = 1, UFB = 79%, SH-aLRT = 74.4%) and M (PP = 0.97, UFB = 67%, SH-aLRT = 65.8%) diverge. Clade J includes two sister groups: the 'marmoratus group' (clade K, PP = 1, UFB = 99%, SH-aLRT = 97.2%) and the 'hopei group' (clade L, PP = 1, UFB = 100%, SH-aLRT = 100%). The 'marmoratus group' contains *G. laevis* Kulzer and *G. marmoratus* Waterhouse (PP = 1, UFB = 100%, SH-aLRT = 99.8%) as sisters to *G. maculatus* Guerrero & Aceituno and *G. curtisi* Fairmaire. The 'hopei group' includes *G. hopei* and *G. peniciliger* Gebien (PP = 1, UFB = 98%, SH-aLRT = 97.8%) as sisters to *G. foveopunctatus* from Cuesta el Espino (see Figure 3, loc. 32) and Los Pozos (see Figure 3, loc. 33) and *G. leechi* Kulzer, *G. coriaceus* from northern Huentelauquen (see Figure 3, loc. 34), *G.* aff. *paulseni* from El Palqui (see Figure 3, loc. 29), La Cisterna (see Figure 3, loc. 31), Peaje Canela (see Figure 3, loc. 34) and Quendaño (see Figure 3, loc. 34) + remaining specimens of *G. laevigatus* + *G. paulseni* Fairmaire from Cuesta Cavilolen (see Figure 3, loc. 36) + *G. modestus* Kulzer from Mincha Sur (see Figure 3, loc. 35) and Los Vilos (see Figure 3, loc. 36), all nodes/branches with high support (PP = 1, UFB = 100%, SH-aLRT = 83.3–99.7%).

Clade M separates into two groups: the 'pumilus group' (clade N, PP = 1, UFB = 100%, SH-aLRT = 100%) as sister to the clade O (PP = 0.9, UFB = 100%, SH-aLRT = 98.8%). The 'pumilus group' includes *G.* aff. *modestus* from Peaje Canela (see Figure 3, loc. 34) and *G. pumilus* Kulzer. Clade O includes the last two main groups: 'parvus group' (clade P, PP = 1, UFB = 90%, SH-aLRT = 70.4%) and 'luczotii group' (clade Q, PP = 1, UFB = 100%, SH-aLRT = 99.9%). The 'parvus group' contains several species and splits into (*G. atacamensis* Fairmaire + *G. parvus* Solier) (PP = 0.9, UFB = 98%, SH-aLRT = 87.3%) + *G. amabilis* Kulzer and *G. barriai* Kulzer (PP = 1, UFB = 100%, SH-aLRT = 98.8%), with this subclade as a sister to *G. planatus* Solier + (*G. kulzeri* Peña + *G. planicollis* Gebien) + (*G. camanchaca* Zúñiga-Reinoso, Pinto & Predel + *G. chango* Mondaca) (PP = 1, UFB = 97%, SH-aLRT = 95.7%). Finally, within the 'luczotii group', several species are present, with *G. angustus* Philippi & Philippi + *G. batesi* Fairmaire being the first to diverge from the rest (PP = 1, UFB = 99%, SH-aLRT = 99.3%). Following this, *G. kingi* Reed from Los Toyos (see Figure 3, loc. 11) + *G. subrugatus* Fairmaire, the remaining *G. kingi* specimens and several *G.* aff. *kingi* from Freirina (see Figure 3, loc. 14) and Guacolda (see Figure 3, loc. 13), form a sister clade to the remaining species (PP = 1, UFB = 95%, SH-aLRT = 98.8%). The clade comprising five lineages of *G. crispaticollis* Fairmaire, *G. luczotii* and *G. multigranulosus* Pizarro-Araya & Flores is a sister clade (PP = 1, UFB = 100%, SH-aLRT = 99.7%) to the group containing *G. gebieni* Kulzer from Carrizalillo (see Figure 3, loc. 18), *G. confusus* Guerrero & Vidal from Quebrada Chanaral (see Figure 3; loc. 16) and *G. elongatus* Waterhouse + *G. penai* Kulzer + (*G. gebieni* from Aguada Tongoy (see Figure 3, loc. 15) + (*G. whitei* Waterhouse from Espantajos (see Figure 3, loc. 18) + (remaining *G. confusus* and remaining *G. whitei*) (PP = 0.82, UFB = 88%, SH-aLRT = 28.7%). The ML tree was in general quite similar to the BI tree except for the position of the clade B, F and H in which clade B is sister to clade D; subsequently, clade F is sister to clade B and D and clade F is the first to separate from the rest of *Gyriosomus* (Figure S1).

Molecular species delimitation

In general, molecular species delimitation analyses identify more species than those proposed by classical taxonomy in our study (i.e., 41 species).

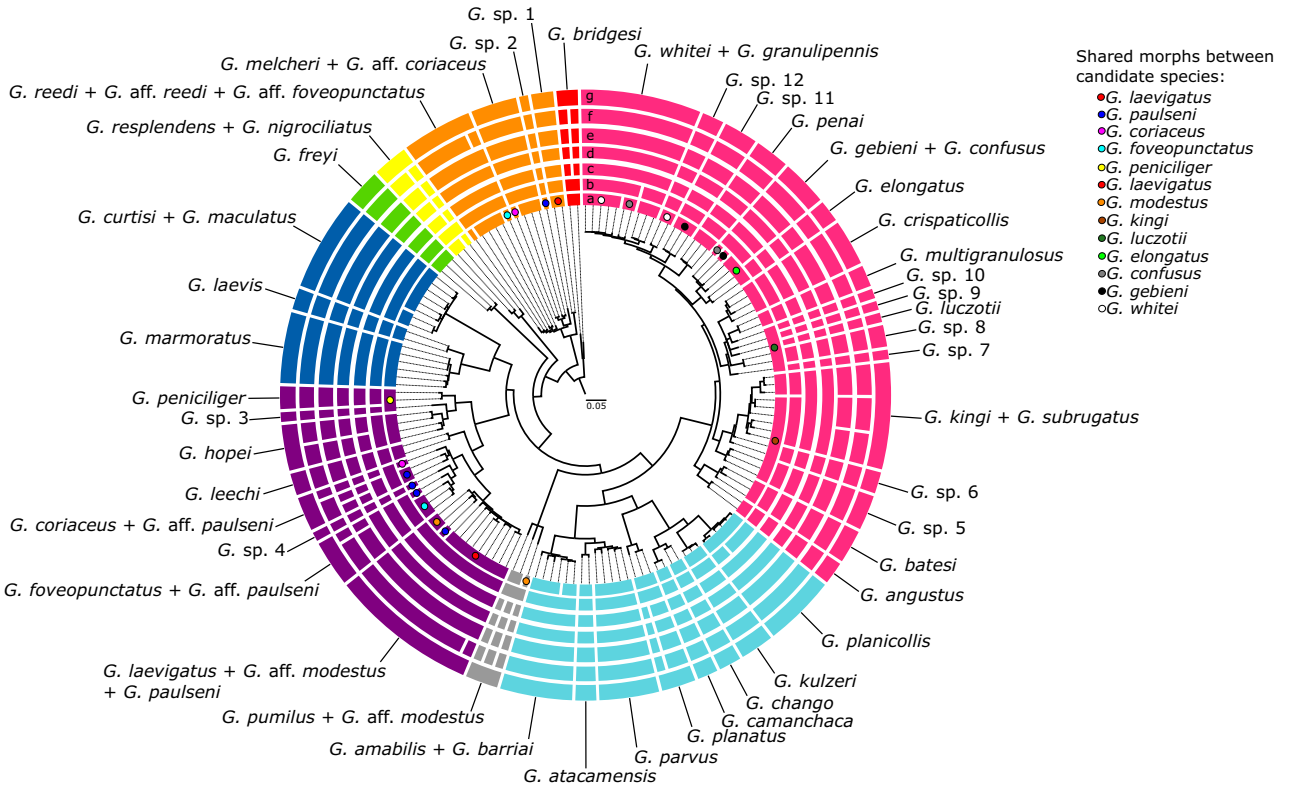

FIGURE 4 Summary of the different species delimitation hypotheses included in this study for the genus *Gyriosomus*. The circular bands surrounding the phylogeny represent the results of the delimitation based on different methods. (a) Classical taxonomy; (b) ABGDr analysis; (c) ASAP analysis; (d) PTP-based analyses with BI tree; (e) PTP-based analyses with ML tree; (f) GMYC analysis; (g) STACEY lumping proposal. Species joined by a plus sign represent STACEY lumping groups, suggesting potential synonymies. To the right, shared morphs between candidate species are indicated by a coloured circle, showing its position in the phylogeny.

PTP-based methods (sPTP and bPTP) yielded highly consistent results, identifying 54 candidate species with the ML tree and 53 with the BI tree. GMYC, the other tree-based approach, proposed 57 candidate species. For the distance-based approach, ASAP identified 52 candidate species; meanwhile, ABGDr identified only 46 candidate species. Additionally, there are differences in the candidate species delimited by the delimitation methods (see Figure 4 and Table S6). Between the species delimitation consensus ('lumping' with 45 candidate species vs. 'splitter' with 55 candidate species), STACEY supported with a 75.2% count fraction value the 'lumping' scenario (instead of the suboptimal 71.7% for 'splitter'). The 'lumping' scenario proposes complete agreement between analyses, revalidating 21 of the 41 species formally described and included in this study: *G. angustus*, *G. atacamensis*, *G. batesi*, *G. bridgesi*, *G. camanchaca*, *G. chango*, *G. crispaticollis*, *G. elongatus*, *G. freyi*, *G. hopei*, *G. kulzeri*, *G. laevis*, *G. leechi*, *G. luczotii*, *G. marmoratus*, *G. multigranulosus*, *G. parvus*, *G. penai*, *G. peniciliger*, *G. planatus* and *G. planicollis* (see Figure 5).

Twelve of the remaining candidate species are considered new species, of which formal description based on morphology is the subject of a follow-up study, including *G.* sp. 1 (from Machalí, spot 43), *G.* sp. 2 (from Canela, spot 34), *G.* sp. 3 (from Socos, spot 27), *G.* sp. 4 (from Palqui, spot 29), *G.* sp. 5 (from Guacolda, spot 13), *G.* sp. 6 (from Los Toyos, spot 11), *G.* sp. 7 (from La Higuera, spot 21), *G.* sp. 8 (from Cuesta Buenos Aires, spot 21), *G.* sp. 9 (from Las Tacas, spot 23), *G.* sp. 10 (from Tabaqueros, spot 25), *G.* sp. 11 (from Aguada de Tongoy, spot 15) and *G.* sp. 12 (from Espantajos, spot 18) (see Figure 5). All those delimited entities have more than 2.0% genetic distance from the phylogenetically closest species (minimum delimitation distance = 2.1% and maximum delimitation distance = 6.2%, see Table S7).

Finally, there are 12 candidate species for synonymy (see Figure 5). In the 'reedi group', the analyses recognize two candidate species for synonymy: *G.* aff. *coriaceus* would be a junior synonym of *G. melcheri* and the other is *G. reedi*, which includes the morph *G.* aff. *foveopunctatus* from Soruco (see Figure 3, loc. 31) plus *G.* aff. *reedi*. According to the analyses, the 'resplendens group' would be a single species comprising *G. resplendens*, which would be the senior synonym of *G. nigrociliatus*. For the 'marmoratus group', the analyses could identify as candidate species for synonymy the species *G. curtisi*, where *G. maculatus* would be the junior synonym. For the 'hopei group', three candidate species for synonymy are identified; the first includes *G. laevigatus*, which would be the senior synonym of *G. modestus* and *G. paulseni*. The others are the specimens identified as *G.* aff. *paulseni*, where some were placed together with *G. foveopunctatus* and others with *G. coriaceus*. For the 'pumilus group' represented by one species, comprises the taxonomical species *G. pumilus*, including the *G.* aff. *modestus* morph from Peaje Canela (see Figure 3, loc. 34). Within the 'parvus group', the analyses recover a single

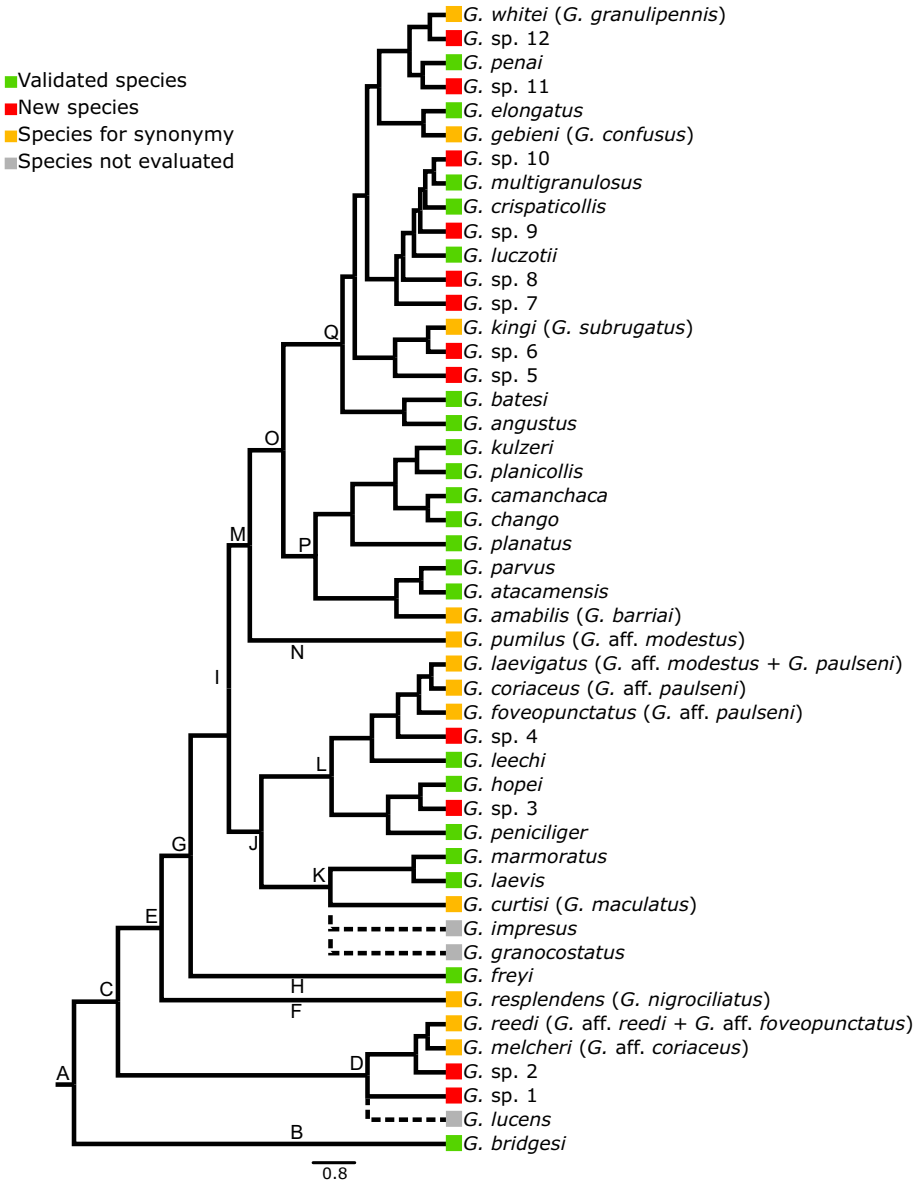

FIGURE 5 Summary of the new systematic proposal for *Gyriosomus* genus based on our results and analyses. The status of each evaluated species is highlighted with a coloured square. Green, validated species; red, new candidate species; orange, candidate species for synonymy and or morph grouping (in brackets the species/morphs included in the unit) and grey; species not evaluated in this study (tentative relationships to main groups are represented with dashed lines). Clades are labelled according to the branches in Figure 3.

candidate species for synonymy, where *G. amabilis* would be the senior synonym of *G. barriai*. Finally, within the 'luczotii group', there are three candidate species consisting of more than one taxonomical species: the first would include *G. kingi* with *G. subrugatus* as a junior synonym; the second comprises *G. gebieni*, which would be the senior synonym of *G. confusus* (see Figure 3, loc. 16); and the third would consist of *G. whitei* with *G. granulipennis* as a junior synonym.

Ecological observations

Our sampling covered the entire known distribution range of *Gyriosomus*, from Paposo to Machalí, and from sea level up to over 3000 m asl (Table S1). Only collections made in 1997, 2002, 2004, 2006, 2009, 2014, 2015, 2023 and 2024 were associated with El Niño events (see intensity in Table S5). Collections from other years (i.e., 1999, 2000, 2001, 2003, 2005, 2007, 2008, 2010, 2011, 2017, 2020, 2021 and 2022) were associated with La Niña or common years (see intensity in Table S5). Across the latitudinal range of *Gyriosomus*, a region of high species diversity is observed between 30.5° S and 31.5° S (Figure 3). In this area, 19 of the 44 described species are recorded. From this zone, the diversity of *Gyriosomus* gradually decreases towards both the north and south, with only one species (*G.* sp. 1) at the southern extreme (~34° S) and three (*G. angustus*, *G. camanchaca* and *G. curtisi*) at the northern extreme (~25° S). Additionally, diversity declines with altitude, with only two species

occurring above 3000 m asl (*G.* aff. *marmoratus* and *G. impressus*). Within this extensive distribution range, the sampled environments were highly contrasting. Some species preferred dunes or loose soil environments with minimal vegetation cover, such as *G. batesi*, *G. elongatus*, *G. gebieni*, *G. kingi* (except for *G. subrugatus* morph), *G. kulzeri*, *G. planicollis*, *G. whitei* (except for *G. granulipennis* morph), *G.* sp. 5, *G.* sp. 6 and *G.* sp. 11 (see Figure 1b,c). Other species favoured alluvial terraces with more compact soils and higher vegetation cover, including *G. camanchaca*, *G. curtisi*, *G. maculatus* (see Figure 1a) and *G. penai*. *G. amabilis*, *G. angustus*, *G. atacamensis*, *G. chango* and *G. parvus* preferred environments similar to those mentioned above but located on slopes and/or plateaus of hills (see Figure 1a,e). A preference for loose soils with a high vegetation cover was also observed for species such as *G. bridgesi*, *G. hopei*, *G. multigranulosus*, *G. peniciliger* and *G.* sp. 3 (see Figure 1d). Additionally, some species showed a preference for grassland, including *G. freyi*, *G. laevigatus*, *G. melcheri*, *G. resplendens*, *G.* sp. 2 and *G.* sp. 4 (see Figures 1h and 2a). We also found carcasses of *G.* aff. *marmoratus* in a high-altitude spiny scrub environment above 3000 m asl in the Elqui Cordillera (29.25° S, 70.32° W) (see Figure 1f).

The distribution ranges of species varied widely. Some species, such as *G. batesi*, *G. curtisi*, *G. hopei* and *G. laevigatus*, exhibit broad distribution ranges (>100 km). In contrast, other species, like *G. atacamensis*, *G. camanchaca*, *G. chango* and *G. kulzeri*, were found within very restricted ranges (<5 km). Most individuals were sampled during the day, with peak activity in the late morning. By midday, individuals were refuged under plants and rocks or buried themselves (Figure 2b,c). On cloudy days, fewer individuals were active, though this activity persisted around midday. Activity generally resumed in the afternoon, with a significant decline occurring before sunset. However, some species, such as *G. curtisi*, *G. marmoratus* and *G.* sp. 11, were recorded as active even at midday and early afternoon. Additionally, species like *G. elongatus*, *G. gebieni*, *G. hopei* and *G. planicollis* were observed active even towards sunset. We particularly observed *G. elongatus* during the last hours of daylight (see Supporting Information V1). Females buried themselves earlier, while males continued to wander, searching for females and even copulating with partially buried females. We also noted male competition for mating with the same female (see Supporting Information V1). Additionally, for *G. camanchaca*, *G. foveopunctatus*, *G. laevigatus*, *G. leechi*, *G. reedi*, *G.* sp. 2 and *G.* sp. 4, we recorded male courtship behaviours, where males performed 'massages' with their prothoracic legs on the elytra of females (see Figure 2d,l and Supporting Information V1). During the entire sampling period, specimens were most frequently observed consuming plant detritus, followed by live plants and occasionally bird and mammal droppings, vertebrate and invertebrate carrion, and even engaging in cannibalism (see examples in Figure 2e–h). The highest density of individuals was noted in areas where the flowering season had ended and annual plants were wilting (Figure 2a,i). Under these conditions, high densities of up to 4–12 individuals per square metre were observed in some species, such as *G. camanchaca*, *G. elongatus*, *G. gebieni*, *G. kingi*, *G. kulzeri*, *G. luczotii*, *G.* sp. 2, *G.* sp. 4, *G.* sp. 5, *G.* sp. 6, *G.* sp. 7, *G.* sp. 8, *G.* sp. 9 and *G.* sp. 10, which were frenetically foraging for food and mates (see Figure 2a,i and Supporting Information V1). Additionally, in some coastal areas where species coexisted sympatrically, interspecific copulation was observed, with *G. gebieni* copulating with *G. whitei*, *G. kulzeri* mating with *G.* sp. 5 and *G. camanchaca* attempting to copulate with *G. curtisi* (see as example Figure 2j–l).

DISCUSSION

Into morphology and genetic species-group exploration

This study represents the first genetic investigation of the extensive diversity within *Gyriosomus*. The nine clades discovered in both phylogenetic reconstructions represent the first attempt to subdivide the *Gyriosomus* genus (see dichotomous key in Table S8). However, the incorporation of missing taxa or improved sampling in the southern range of the genus distribution could help improve the inconsistencies among the reconstructed trees, particularly in their early-diverging relationships. Members of the nine clades exhibit some affinity with each other, as they share many morphological traits, leading to similar body appearances. Thus, we divided them into the groups 'bridgesi', 'freyi', 'hopei', 'luczotii', 'marmoratus', 'parvus', 'pumilus', 'reedi' and 'resplendens'. Consequently, it is possible to assign species to one of these groups based on general morphology alone. Therefore, morphology appears to have a phylogenetic signal only at the clade level. When delineating species within the same clade, this is not the case. Our results indicate that external morphology successfully identified less than 50% of the species suggested by the analyses (see Figure 5). We think that other, less traditional morphological characteristics for this group, such as male and female genitalia, might better define *Gyriosomus* species. These characters have proven valuable in distinguishing phylogenetically close species (Guerrero et al., 2023; Zúñiga-Reinoso et al., 2019).

In this context, the discrepancy between external morphology and the species estimated in our study could be explained by various factors. Historically, the taxonomy of *Gyriosomus* has been studied using external morphological characters, particularly the elytral pattern composed of velvety and waxy white spots, as well as the texture of the pronotum and elytral margins (e.g., Guerrero & Aceituno, 2020; Guerrero & Vidal, 2018; Pizarro-Araya & Flores, 2004). However, based on our results and observations, these morphological characters are often too plastic to be useful as diagnostic tools in taxonomy. The presence or absence of these characters may be due to clines in lineage distribution. The taxonomists identified these clines as different species, but they might represent latitudinal or altitudinal variations within a single species. For example, in the 'reedi group', the species candidates for synonymy of *G. reedi* include the morph *G.* aff. *foveopunctatus* and *G.* aff. *reedi*, which is defined by elongated spots on the side of the elytra. These spots can be present, attenuated or absent, depending on the species. These patterns are unique to each locality, showing morphological variability between populations in a latitudinal cline, where the spots diminish with increasing latitude. Such clines

are also observed in other groups, such as the 'marmoratus group'. For example, *G. curtisi*, which is almost smooth with two to three white velvety linear spots on the elytra, shows a latitudinal trend where the elytral punctures increase and the lateral spots diminish towards the southern end of its distribution. This results in the morph *G. maculatus*, which has strongly punctate elytra and lacks the velvety spots.

In the 'parvus group', an altitudinal cline occurs between the species *G. amabilis* and the *G. barriai* morph. Males of the morph *G. barriai* have half of the elytra covered by a single extensive and uninterrupted white velvety spot, show an elevation of striae interrupting the velvet towards more inland places, and males of the morph *G. amabilis* show 4–5 diagonal white velvety linear spots on the elytra. In the 'hopei group', a series of clines is observed, with three independent candidate species sharing the *G. paulseni* morph: the first unit groups this morph with *G. foveopunctatus*, the second includes *G. laevigatus* and *G. modestus* and the third includes *G. coriaceus*. This series of clines occurs within the Zone of High Cladistic Sympatry (ZHCS, Figure 3), exacerbating the species diversity within this zone and reflecting both altitudinal and latitudinal gradients. The extent of this phenomenon leads us to classify these clines as polymorphic species candidates for synonymy (see Figure 5), demonstrating the plasticity of some characters widely used in taxonomy, which likely represent local adaptations to environmental gradients (Huxley, 1938). It is important to emphasize that all identified clines (i.e., candidate species with different morphs) exhibit genetic distances of less than 2% in the COI gene, indicating no significant genetic differentiation within each species (see Table S7).

Rearrangement proposal for *Gyriosomus*

From the 12 candidate species for synonymy, four are morphs for which a precise identification is not possible, and their identity was assigned according to morphological affinity (see Figure 5 for *G. coriaceus*, *G. foveopunctatus*, *G. pumilus* and *G. reedi*). However, the other synonymies incorporate well-identified taxonomic entities. Morphologically and genetically, these synonymies appear to be well supported. The most obvious examples of these synonymies are those suggested for *G. amabilis*, *G. gebieni*, *G. kingi*, *G. laevigatus* and *G. resplendens*. This is because the species to be synonymized are morphologically very similar (with only minor differences in size and/or pronotal/elytral pattern) and genetically showed very low variability (<0.5%, see Table S7). A particular case is that between *G. granulipennis* and *G. whitei* should be considered; the genetic distance between entities is about 1% (see Table S7), and both entities are geographically isolated, as *G. granulipennis* only inhabits Choros Island, which is about 5 km from the mainland. Also, morphologically they differ quite a lot, so we suggest here to downgrade *G. granulipennis* to the subspecies level: *G. whitei granulipennis*.

Finally, we suggest that the 12 candidate species should be considered as new species by adding new characters, as mentioned above in the previous section. An exhaustive review of morphological characters that could be used as diagnostics is being carried out by a part of the co-authors (i.e., M. G. and V. M. D.); thus, a formal description of these species will be made in the near future together with a taxonomic revision of this genus. For example, the species *G.* sp1, *G.* sp2, *G.* sp5, *G.* sp7 and *G.* sp9 show a greater combination of characters that differentiate them from morphologically related species (i.e., *G. laevigatus*, *G. hopei*, *G. kingi* and *G. luczoti*, respectively). In this case, the pronotal disc shape, the pronotal margin shape, elytral margin shape, elytral roughness and elytral margin pilosity appear to be informative external characters, in addition to genitalia shape. However, the other seven species need to be studied in more detail because of their high similarity to other species and/or a larger number of specimens to understand intraspecific variation is needed. Our new proposal is summarized in Figure 5 for a better understanding.

Cryptic species and possible hybridization cases

On the other hand, the taxonomy of *Gyriosomus* is even more complex, as there are cases of convergence and/or cryptic phenomena, a phenomenon already reported for other Nycteliini in the region (see Zúñiga-Reinoso & Méndez, 2018). For example, the clade comprising *G. crispaticollis*, *G. luczotii*, *G. multigranulosus*, *G.* sp. 7, *G.* sp. 8, *G.* sp. 9 and *G.* sp. 10 (closely related to *G. luczotii*) is a clear case of a group of cryptic species. The morphological species within this group are so similar that *G. crispaticollis* was considered a synonym of *G. luczotii* until 2023 (Guerrero et al., 2023). The remaining candidate species with *G. luczotii* morph exhibit a clear latitudinal genetic structure with a high degree of morphological similarity, leading to their consideration as a single entity (see Figure 5). A similar pattern was also found for the *G. kingi* and *G. peniciliger* complexes (see Figures 3 and 5). Given their common origin, it is expected that this phylogenetic proximity explains the high level of morphological similarity or cryptic appearance (Struck et al., 2018), which complicates taxonomic studies of these groups.

Alternatively, cryptic appearances might arise because the taxonomic characters, being highly plastic, could be expressed as homoplasies. Thus, different lineages might converge on the same morphology when adapting to and colonizing similar environments (Zúñiga-Reinoso & Méndez, 2018). We have identified cases of convergence and cryptic appearance between distantly related groups (i.e., 'reedi group' = clade D and 'hopei group' = clade L), which independently acquire the morphs of *G. coriaceus*, *G. foveopunctatus*, *G. laevigatus* and *G. paulseni*. Both groups seem to converge on similar morphologies when inhabiting comparable environments and tend to be very similar. This example of convergent morphologies also involves clades with polymorphic candidate species, which are more likely to resemble each other due to the plasticity of their components.

A special case involves the species located in the dune systems of Punta de Choros and Aguada de Tongoy (28.5° S–29° S, see Figure 3 loc. 15–19). According to our analyses, this region is inhabited by six

candidate species living in sympatry that share a common ancestor. It suggests that the common ancestor colonized the area and diversified in situ. Three taxonomical species within this subclade exhibit similar morphologies (i.e., *G. confusus*, *G. elongatus*, *G. gebieni*; see Guerrero & Vidal, 2018), which show signs of COI gene exchange, but this also occurs between morphologically very dissimilar species (i.e., *G. whitei*). Our results imply that genetic exchange may still be happening between nearby but genetically distinct populations (over 2.5% genetic distance). This suspicion is reinforced by observations of copulation between different morph/species inhabiting this area (see Figure 2j). This phenomenon of species consisting of various morphologies and showing signs of hybridization has also been hypothesized for buprestids (i.e., *Ectinogonia* Spinola: Dicercini) that cohabit the same dunes in Punta de Choros with *Gyriosomus* (Anguita-Salinas et al., 2022). This indicates that this area could promote genetic differentiation, yet the lineages still recognize each other reproductively. However, this hypothesis needs to be properly tested in future studies.

Distribution and habitat

Our sampling covered the entire distribution range of *Gyriosomus* and included nearly all species except *G. granocostatus*, *G. impressus* and *G. lucens*, which are described from localities with difficult access, doubtful type localities and/or are rare in nature (see for example Guerrero & Aceituno, 2020; Pizarro-Araya et al., 2012). Habitat specialization promotes the group's diversity, as evidenced by the various preferences recorded with morphological differentiation. Some species demonstrated a high degree of specialization towards specific habitats, such as the dune-dwelling species *G. batesi*, *G. elongatus*, *G. gebieni*, *G. kingi*, *G. kulzeri*, *G.* sp. 5, *G.* sp. 6 and *G.* sp. 11, which were often found on sandy plains at the foot of the dunes and are characterized by elongated bodies with significant or abundant pilosity. Meanwhile, species specialized in compacted soils, such as *G. atacamensis*, *G. camanchaca* and *G. penai*, were found on solid soil plains with sparse vegetation characterized by small body size. Additionally, the mountain species *G. granocostatus* and *G. impressus* have been described in mountainous environments with limited shrub vegetation and rocky soils, easily recognized by their big globose bodies with sparse tiny white dots over the elytra (see Guerrero & Aceituno, 2020). Generally, these specialist species are also known for being present in very restricted areas.

In contrast, some species appear more generalist, capable of being found in various habitats throughout their distribution ranges. It is the case for *G. curtisi*, *G. hopei*, *G. laevigatus* and *G. marmoratus*. These species can be found interchangeably on hillside slopes, coastal plains or inland areas with loose or compacted soils. Our record of *G.* aff. *marmoratus* carcasses from the Elqui Cordillera confirms this species' ability to inhabit high-altitude environments. This record would increase the number of species in high mountain environments, as only *G. impressus* had been documented above 3000 m in the Copiapó Cordillera (Guerrero & Aceituno, 2020). Another notable generalist species is the newly defined *G. curtisi*, which has one of the broadest distribution ranges among *Gyriosomus* species, with records extending from Paposo (24.8° S, see Figure 3, loc. 1) to Carrizal Bajo (28.49° S, see Figure 3, loc. 10), covering more than 300 km. All the observations mentioned above align with the findings of Vidal and Guerrero (2007) and suggest that *Gyriosomus* is an ecologically diverse group.

Our different observations of daily activities align with Vidal et al. (2011) and Tirado et al. (2018), who demonstrated that the activity of *Gyriosomus* is likely regulated by temperature, avoiding exposure during the hottest hours of the day. Additionally, many diurnal desert tenebrionids seek refuge at dusk due to their intrinsic biological activity clock and the lower temperatures that impact ectothermic animals (Cloudsley-Thompson, 2001). Conversely, we observed that *Gyriosomus* takes advantage of coastal cloud cover to extend its activity during the hottest hours on some days, and it may remain active until the late afternoon. The season for these tenebrionids typically spans from September to November, but we recorded three active adults of *G.* sp. 6 in February 2021 that were captured in pitfall traps in the Guacolda area (28.5° S, see Figure 3, loc. 13). During periods of high activity across their entire distribution range, it is frequent to observe *Gyriosomus* feeding on various available food sources, indicating they are generalist and opportunistic feeders, which also includes cannibalism (see Figure 2h). These observations are somewhat similar to those recorded by Mondaca (2004) and Pizarro-Araya (2010).

Landscape and climate phenomena, potential key factors for diversification

As described in other studies, the group prefers coastal environments and interior plains of the intermediate depression (Pizarro-Araya & Jeréz, 2004). Some species can reach high population densities in these habitats, as we observed for several species with five to 12 individuals per square metre (see Figure 2a,i and Supporting Information V1). It surpasses the observations of Peña (1959), who reported high densities with four individuals per square metre. The richness distribution in *Gyriosomus* follows both a latitudinal and an altitudinal gradient, with higher diversity in low-altitude areas between 30.5° S and 31.5° S. Diversity decreases both to the north and south and with increasing altitude. This significantly reduces the high-richness zones previously identified by Pizarro-Araya and Jeréz (2004). The high-diversity pattern is likely due to the convergence of species from different clades around 30.5° S–31.5° S in the ZHCS (see Figure 3). This area shows a spatial resemblance to diversity patterns of other beetles in the region (see Anguita-Salinas et al., 2022; Peña, 1966a). Vegetationally, this zone is described as Steppic Shrubland and represents the transition between the Mediterranean Shrubland and the Atacama Desert (Luebert & Pliscoff, 2017). We hypothesize that the high diversity of *Gyriosomus* in this area is due to various colonization events and/or vicariance events mediated by the region's irregular topography. As suggested for *Psectrascelis* Solier (Zúñiga-Reinoso et al., 2021), the irregular topography in this area presumably also promotes high habitat heterogeneity, which would favour diversification in *Gyriosomus*.

For example, we have recorded a marked genetic structure within the *G. kingi* complex (*G. kingi*, *G.* sp. 5 and *G.* sp. 6), with candidate species isolated in different dune complexes: Guacolda (see Figure 3, loc. 13), La Gruta (see Figure 3, loc. 11) and Los Toyos (see Figure 3, loc. 11), with the most noticeable barrier being the Huasco River, which separates Guacolda from the rest of the northern riverbank localities by only ~7 km. Similar to *G. kingi*, *G. planatus* also shows a marked genetic structure on both sides of the Huasco River, separating the populations of Aguada de Tongoy (see Figure 3, loc. 15) and Los Toyos (see Figure 3, loc. 11). Additionally, the *G. luczotii* complex (*G. luczotii*, *G.* sp. 7, *G.* sp. 8, *G.* sp. 9 and *G.* sp. 10) also exhibits genetic structure. The five candidate species within this group from La Higuera (see Figure 3, loc. 21), Cuesta Buenos Aires (see Figure 3, loc. 21), Cuesta los Porotitos (see Figure 3, loc. 22), Las Tacas (see Figure 3, loc. 23) and Tabaqueros (see Figure 3, loc. 25) are presumably separated by the numerous deep quebradas (e.g., Quebrada Honda) and rivers (e.g., Río Elqui) that cross the landscape in that region. In line with this, Guerrero et al. (2023) found that *G. crispaticollis* and the *G. luczotii* complex (sister groups) are separated by the Quebrada Seca, which is only about 2 km wide in Tongoy. These and other phylogeographic breaks related to rivers have already been reported for other arthropods in that region (Ceccarelli et al., 2017; Larrea-Meza et al., 2020; Pinto et al., 2022). However, other factors that could be reinforcing the diversification of these beetles should not be ruled out.

These darkling beetles, being flightless, are prone to diversification at a micro-scale (Zúñiga-Reinoso et al., 2021, 2023), which contributes to the high degree of micro-endemism observed (Guerrero & Diéguez, 2018; Mondaca, 2004; Pizarro-Araya et al., 2012; Pizarro-Araya & Jeréz, 2004; Zúñiga-Reinoso et al., 2019). This characteristic has been used to assign conservation categories to some species (Jeréz et al., 2015; Pizarro-Araya et al., 2012). However, it is significant to consider the phenology of these insects, as the mass appearance of *Gyriosomus* adults is often associated with the occurrence of El Niño events, which bring more rainfall than usual and massive blooming (Cepeda-Pizarro et al., 2005a, 2005b). In our case, only collections made in 1997, 2002, 2004, 2006, 2009, 2014 and 2015 align with El Niño years (see Table S5). However, the majority of our observations were made during years influenced by La Niña (i.e., see Table S5), which experienced much localized winter rains that enabled blooming events in patches (see also Guerrero et al., 2023; Zúñiga-Reinoso et al., 2019). In contrast, other La Niña years, such as 2011 and 2017, had more widespread rains that allowed for massive blooming. The year 2011, in particular, had less accumulated precipitation compared to any El Niño year, but with several small rainfall events that triggered more intense blooming events (Chávez et al., 2019). Therefore, since *Gyriosomus* has adapted its demographic dynamics to these irregular precipitation events, we suspect that these events are a factor to consider for understanding the diversification of the group and the reported micro-endemicity. Massive blooming events in the Atacama Desert (during El Niño years or occasionally La Niña) activate a large number of populations across the range of these beetles, increasing the likelihood of contact between them and enabling long-distance migration/dispersal as suggested for the colonization of Paposo by three species of *Gyriosomus* (Zúñiga-Reinoso et al., 2019). However, the localized rains of La Niña years activate only some populations per event, segregating them by phenological differentiation, which may result in an interesting case of ecological speciation through temporal decoupling. It could explain the higher diversity in the ZHCS, as the southern portion of the Atacama Desert is more influenced by 'patchy' rains during La Niña years (see Table S5). In comparison, species inhabiting the northern part of the distribution (i.e., north of the Huasco River) are likely better adapted to endure long periods without rain to complete their metamorphosis.

CONCLUSION

This work is the first extensive systematic study of *Gyriosomus* using molecular tools and covering the known distribution of these darkling beetles. These charismatic beetles inhabit a broad latitudinal range, occupying a wide variety of environments along the western slope of the Andes. Some species are specialists in specific environments with very restricted ranges, while others are more generalist and have broader distributions. The field observations provided new insights into the natural history of these beetles, including feeding behaviours, courtship, interspecific mating and daily activity patterns. Our analyses suggest the existence of 45 species from a genetic perspective, grouped into nine clades. Half of the previously described species were confirmed in our study, while the status of candidate species and suggested synonyms still need to be reviewed. *Gyriosomus* is composed of the 45 evaluated candidate species plus three additional missing species in total, which will need to be assessed in future studies. However, most morphological characters in classical taxonomy (e.g., elytral patterns and pronotal structures) are highly plastic and vary significantly, especially within species complexes that arise from geographic gradients. We refer to these species complexes as polymorphic species. Following our analyses, we also found that the highest diversity along the latitudinal distribution occurs between 30.5° and 31.5° S, an area we refer to as the Zone of High Cladistic Sympatry (ZHCS). This high diversity is attributed to the significant overlap of species from different *Gyriosomus* clades/groups. Several instances of cryptic speciation and convergence were identified among lineages inhabiting similar environments. The observed phylogenetic and distribution patterns, combined with the species rain-dependent phenology and habitat preferences, indicate that topography and ecological factors likely play crucial roles in the group's diversification.

AUTHOR CONTRIBUTIONS

Simón Anguita-Salinas: Conceptualization; data curation; formal analysis; funding acquisition; investigation; methodology; validation; visualization; writing – original draft preparation; writing – review and editing. Marcelo Guerrero: Data curation; investigation; methodology; validation; visualization; writing – review and editing. Víctor M. Diéguez: Data curation; investigation; methodology; visualization; writing – review and editing.

Pablo Pinto: Data curation; investigation; methodology; visualization; writing – review and editing. Sebastián Larrea-Meza: Data curation; investigation; methodology; visualization; writing – review and editing. Alfonso Jara-Flores: Investigation; methodology; writing – review and editing. Reinhard Predel: Conceptualization; funding acquisition; investigation; methodology; project administration; resources; validation; writing – review and editing. Álvaro Zúñiga-Reinoso: Conceptualization; data curation; formal analysis; funding acquisition; investigation; methodology; project administration; resources; supervision; validation; visualization; writing – original draft preparation; writing – review and editing.

ACKNOWLEDGEMENTS

We thank the following colleagues for their support for this study: A. Ramirez-Cuadros (Santiago, Chile) for their pictures in 1 h and field help, V. Villablanca (Valparaiso, Chile) for their pictures 1D (*G. hopei*), 2 h y 2j, R. M. Barahona-Segovia (Valdivia, Chile) and S. Roitman (Santiago, Chile) for the facilitated material. Especially thanks to D. Mardones (Cologne, Germany) for her laboratory and field help and M. Valladares (Santiago, Chile) for his help in the multilocus species delimitation analysis. Special thanks also to the National Forestry Corporation (CONAF, Chile) for sampling permits N° 005/2017, 105/2020 and 016/2022, to the National Research and Development Agenda (ANID, Chile) for the National PhD grant No. 21210453 and the PhD internship abroad second call 2023 and to the International Research Training Group (IRTG) for the IRTG 2022 grant. This study was funded by the Deutsche Forschungsgemeinschaft (DFG, German Research Foundation)—Projektnummer 268236062—SFB 1211. Open Access funding enabled and organized by Projekt DEAL. [Correction added on 24 October 2025, after first online publication: Projekt DEAL funding statement has been added.].

CONFLICT OF INTEREST STATEMENT

The authors declare no conflicts of interest.

DATA AVAILABILITY STATEMENT

The data that support the findings of this study are openly available in CRC1211 Database (CRC1211DB) at https://www.crc1211db.uni-koeln.de/search/view.php?dataID=1034 (Anguita-Salinas & Zúñiga-Reinoso, 2025). All novel genetic data produced for this study are available through NIH genetic sequence database Genbank at https://www.ncbi.nlm.nih.gov/genbank/, with accession numbers of all data given in Table S1.

ORCID

Simón Anguita-Salinas https://orcid.org/0000-0002-2995-7784
Marcelo Guerrero https://orcid.org/0009-0003-4301-084X
Víctor M. Diéguez https://orcid.org/0000-0001-7726-3544
Pablo Pinto https://orcid.org/0000-0002-0247-0976
Sebastián Larrea-Meza https://orcid.org/0000-0001-8066-7515
Alfonso Jara-Flores https://orcid.org/0000-0001-7578-4178
Reinhard Predel https://orcid.org/0000-0002-0202-6672
Álvaro Zúñiga-Reinoso https://orcid.org/0000-0002-7949-081X

REFERENCES

Anguita-Salinas, S., Barahona-Segovia, R.M., Poulin, E. & Zúñiga-Reinoso, Á. (2022) Genetic-morphological uncoupling and crypsis in *Ectinogonia* (Coleoptera: Buprestidae) suggest a complex evolutionary history in these polymorphic jewel beetles from Chile. *Biological Journal of the Linnean Society*, 137, 613–625. Available from: https://doi.org/10.1093/biolinnean/blac075

Anguita-Salinas, S. & Zúñiga-Reinoso, A. (2025) Database of genes and trees used for the manuscript "How many cows are in the desert? Molecular phylogeny and species delimitation of the genus *Gyriosomus* (Coleoptera: Tenebrionidae) from the Atacama Desert". CRC1211 Database (CRC1211DB); https://www.crc1211db.uni-koeln.de/search/view.php?dataID=1034

Arntz, W. & Fahrbach, E. (1996) *El Niño: experimento climático de la naturaleza*. Mexico: Fondo de Cultura Económica, pp. 1–312.

Bouchard, P., Bousquet, Y., Aalbu, R.L., Alonso-Zarazaga, M.A., Merkl, O., & Davies, A.E. (2021) Review of genus-group names in the family Tenebrionidae (Insecta, Coleoptera). *ZooKeys*, 1050, 1–633. Available from: https://doi.org/10.3897/zookeys.1050.64217.

Bouckaert, R., Vaughan, T.G., Barido-Sottani, J., Duchêne, S., Fourment, M., Gavryushkina, A. et al. (2019) BEAST 2.5: an advanced software platform for Bayesian evolutionary analysis. *PLoS Computational Biology*, 15(4), e1006650.

Ceccarelli, F.S., Pizarro-Araya, J. & Ojanguren-Affilastro, A.A. (2017) Phylogeography and population structure of two *Brachistosternus* species (Scorpiones: Bothriuridae) from the Chilean coastal desert–the perils of coastal living. *Biological Journal of the Linnean Society*, 120(1), 75–89. Available from: https://doi.org/10.1111/bij.12877

Cepeda-Pizarro, J., Pizarro-Araya, J. & Vásquez, H. (2005a) Composición y abundancia de artrópodos epígeos del Parque Nacional Llanos de Challe: impactos del ENOS de 1997 y efectos del hábitat pedológico. *Revista Chilena de Historia Natural*, 78(4), 635–650. Available from: https://doi.org/10.4067/s0716-078x2005000400004

Cepeda-Pizarro, J., Pizarro-Araya, J. & Vásquez, H. (2005b) Variación en la abundancia de Artropoda en un transecto latitudinal del desierto costero transicional de Chile, con énfasis en los tenebriónidos epígeos. *Revista Chilena de Historia Natural*, 78(4), 651–663. Available from: https://doi.org/10.4067/s0716-078x2005000400005

Chávez, R.O., Moreira-Muñoz, A., Galleguillos, M., Olea, M., Aguayo, J., Latín, A. et al. (2019) GIMMS NDVI time series reveal the extent, duration, and intensity of "blooming desert" events in the hyper-arid Atacama Desert, northern Chile. *International Journal of Applied Earth Observation and Geoinformation*, 76, 193–203. Available from: https://doi.org/10.1016/j.jag.2018.11.013

Chernomor, O., Von Haeseler, A. & Minh, B.Q. (2016) Terrace aware data structure for phylogenomic inference from supermatrices. *Systematic Biology*, 65, 997–1008. Available from: https://doi.org/10.1093/sysbio/syw037

Cloudsley-Thompson, J. (2001) Thermal and water relations of desert beetles. *Naturwissenschaften*, 88, 447–460. Available from: https://doi.org/10.1007/s001140100256

DeWaard, J.R., Ratnasingham, S., Zakharov, E.V., Borisenko, A.V., Steinke, D., Telfer, A.C. et al. (2019) A reference library for Canadian invertebrates with 1.5 million barcodes, voucher specimens, and DNA samples. *Scientific Data*, 6(1), 308. Available from: https://doi.org/10.1038/s41597-019-0320-2

Drummond, A.J. & Rambaut, A. (2007) BEAST: Bayesian evolutionary analysis by sampling trees. *BMC Evolutionary Biology*, 7, 1–8. Available from: https://doi.org/10.1186/1471-2148-7-214

Flores, G.E. (1997) Revisión de la tribu Nycteliini (Coleoptera: Tenebrionidae). *Revista De La Sociedad Entomológica Argentina*, 56, 1–19. Available from: https://doi.org/10.1664/0028-7199(2000)108[0013:CAOTNT]2.0.CO;2

Flores, G.E. (2000) Cladistic analysis of the neotropical tribe Nycteliini (Coleoptera: Tenebrionidae). *Journal of the New York Entomological Society*, 108(1), 13–25.

Fujisawa, T. & Barraclough, T.G. (2013) Delimiting species using single-locus data and the generalized mixed yule coalescent approach: a revised method and evaluation on simulated data sets. *Systematic Biology*, 62(5), 707–724. Available from: https://doi.org/10.1093/sysbio/syt033

Gebien, H. (1937) Katalog der Tenebrioniden. Teil I. In: *Pubblicazioni del Museo Entomologico Pietro Rossi*. Italia: Museo Entomologico Pietro Rossi, Vol. 2, pp. 505–883.

Gebien, H. (1944) Die Gattung *Gyriosomus* Guér. Coleoptera, Tenebrionidae. *Mitteilungen Der Münchener Entomologischen Gesellschaft*, 34, 135–194.

Guérin-Méneville, F.E. (1834) Matériaux pour une classification des Mélasomes. *Magazine de Zoologie*, 3, 1–39.

Guerrero, M. & Aceituno, G. (2020) Nuevas especies del género *Gyriosomus* Guérin-Méneville (Coleoptera: Tenebrionidae: Nycteliini) de Chile, y nuevo estatus para *Gyriosomus faveopunctatus laevis* Kulzer. *Revista Chilena de Entomología*, 46(2), 277–290. Available from: https://doi.org/10.35249/rche.46.2.20.18

Guerrero, M. & Diéguez, V.M. (2018) Redescubrimiento de *Gyriosomus kulzeri* Peña (Tenebrionidae: Nycteliini): una especie poco conocida del Desierto de Atacama, Chile. *Revista Chilena De Entomología*, 44(1), 9–13.

Guerrero, M., Diéguez, V.M., Anguita-Salinas, S. & Zúñiga-Reinoso, Á. (2023) The discarded cow from the flowered desert: revalidation of *Gyriosomus crispaticollis* Fairmaire, 1886 stat. rev. (Coleoptera: Tenebrionidae) in Southern Atacama, Chile. *Zootaxa*, 5319, 283–291. Available from: https://doi.org/10.11646/zootaxa.5319.2.9

Guerrero, M. & Vidal, P. (2018) Nueva especie del género *Gyriosomus* Guérin-Méneville (Tenebrionidae: Nycteliini) de Chile. *Revista Chilena de Entomología*, 44(1), 93–98.

Guindon, S., Dufayard, J.F., Lefort, V., Anisimova, M., Hordijk, W. & Gascuel, O. (2010) New algorithms and methods to estimate maximum-likelihood phylogenies: assessing the performance of PhyML 3.0. *Systematic Biology*, 59(3), 307–321. Available from: https://doi.org/10.1093/sysbio/syq010

Hall, T.A. (1999) BioEdit: a user-friendly biological sequence alignment editor and analysis program for windows 95/98/NT. *Nucleic Acids Symposium Series*, 41, 95–98.

Hoang, D.T., Chernomor, O., Von Haeseler, A., Minh, B.Q. & Vinh, L.S. (2018) UFBoot2: improving the ultrafast bootstrap approximation. *Molecular Biology and Evolution*, 35(2), 518–522. Available from: https://doi.org/10.1093/molbev/msx281

Huxley, J. (1938) Clines: an auxiliary taxonomic principle. *Nature*, 142(3587), 219–220. Available from: https://doi.org/10.1038/142219a0

Jeréz, V., Zúñiga-Reinoso, Á., Muñoz-Escobar, C. & Pizarro-Araya, J. (2015) Acciones y avances sobre la conservación de insectos en Chile. *Gayana (Concepción)*, 79(1), 1–3. Available from: https://doi.org/10.4067/s0717-65382015000100001

Jones, G.R. (2017) Algorithmic improvements to species delimitation and phylogeny estimation under the multispecies coalescent. *Journal of Mathematical Biology*, 74(1), 447–467. Available from: https://doi.org/10.1007/s00285-016-1034-0

Kalyaanamoorthy, S., Minh, B.Q., Wong, T.K., Von Haeseler, A. & Jermiin, L.S. (2017) ModelFinder: fast model selection for accurate phylogenetic estimates. *Nature Methods*, 14, 587–589. Available from: https://doi.org/10.1038/nmeth.4285

Kumar, S., Stecher, G., Li, M., Knyaz, C. & Tamura, K. (2018) MEGA X: molecular evolutionary genetics analysis across computing platforms. *Molecular Biology and Evolution*, 35, 1547–1549. Available from: https://doi.org/10.1093/molbev/msy096

Lanfear, R., Frandsen, P.B., Wright, A.M., Senfeld, T. & Calcott, B. (2017) PartitionFinder 2: new methods for selecting partitioned models of evolution for molecular and morphological phylogenetic analyses. *Molecular Biology and Evolution*, 34, 772–773. Available from: https://doi.org/10.1093/molbev/msw260

Larrea-Meza, S., Pinto, P., Collado, G. & Zúñiga-Reinoso, Á. (2020) A new species of *Psectrascelis* (Coleoptera: Tenebrionidae: Pimeliinae) from the coastal dunes of the Atacama Desert, Chile. *Zootaxa*, 4845(1), 109–118. Available from: https://doi.org/10.11646/zootaxa.4845.1.8

Luebert, F. & Pliscoff, P. (2017) *Sinopsis bioclimática y vegetacional de Chile*, 2nd edition. Chile: Editorial Universitaria.

Mondaca, J. (2004) Nueva especie de *Gyriosomus* Guérin-Méneville, 1834 (Coleoptera: Tenebrionidae: Nycteliini) del extremo norte de la Región de Atacama (Chile). *Revista Chilena De Entomología*, 30, 21–26.

Nguyen, L.T., Schmidt, H.A., Von Haeseler, A. & Minh, B.Q. (2015) IQ-TREE: a fast and effective stochastic algorithm for estimating maximum-likelihood phylogenies. *Molecular Biology and Evolution*, 32(1), 268–274. Available from: https://doi.org/10.1093/molbev/msu300

Peña, L.E. (1959) Las vaquitas del desierto. *Noticiero Mensual Del Museo Nacional De Historia Natural (Chile)*, 37, 2.

Peña, L.E. (1966a) A preliminary attempt to divide Chile into entomofaunal regions, based on the Tenebrionidae (Coleoptera). *Postilla*, 97, 1–17.

Peña, L.E. (1966b) Catálogo de los Tenebrionidae (Coleoptera) de Chile. *Entomologische Arbeiten Aus Dem Museum G. Frey*, 17, 397–453.

Pinto, P., Larrea-Meza, S. & Zúñiga-Reinoso, Á. (2022) A new species of *Diastoleus* Solier (Coleoptera: Tenebrionidae) from the hyperarid Andes of the Atacama Desert of Chile. *Annales Zoologici*, 72(1), 91–96. Available from: https://doi.org/10.3161/00034541anz2022.72.1.006

Pizarro-Araya, J. (2010) Hábitos alimenticios del género *Gyriosomus* Guérin-Méneville, 1834 (Coleoptera: Tenebrionidae):¿ Qué comen las vaquitas del desierto costero? *IDESIA*, 28, 115–119. Available from: https://doi.org/10.4067/s0718-34292010000300015

Pizarro-Araya, J. & Flores, G.E. (2004) Two new species of *Gyriosomus* Guérin-Méneville from the Chilean coastal desert (Coleoptera: Tenebrionidae: Nycteliini). *Journal of the New York Entomological Society*, 112, 121–126. Available from: https://doi.org/10.1664/0028-7199(2004)112[0121:tnsogg]2.0.co;2

Pizarro-Araya, J. & Flores, G.E. (2006) La posición sistemática de *Geoborus lineatus* comb. nov. (ex. *Gyriosomus*) (Coleoptera: Tenebrionidae). *Revista De La Sociedad Entomológica Argentina*, 65, 93–98.

Pizarro-Araya, J. & Jeréz, V. (2004) Distribución geográfica del género *Gyriosomus* Guérin-Méneville, 1834 (Coleoptera: Tenebrionidae): una aproximación biogeográfica. *Revista Chilena de Historia Natural*, 77, 491–500. Available from: https://doi.org/10.4067/S0716-078X2004000300008

Pizarro-Araya, J., Vergara, O.E. & Flores, G.E. (2012) *Gyriosomus granulipennis* Pizarro-Araya & Flores 2004 (Coleoptera: Tenebrionidae): Un caso extremo a conservar. *Revista Chilena de Historia Natural*, 85(3), 345–349. Available from: https://doi.org/10.4067/s0716-078x2012000300009

Puillandre, N., Brouillet, S. & Achaz, G. (2021) ASAP: assemble species by automatic partitioning. *Molecular Ecology Resources*, 21(2), 609–620. Available from: https://doi.org/10.1111/1755-0998.13281

Puillandre, N., Lambert, A., Brouillet, S. & Achaz, G. (2012) ABGD, automatic barcode gap discovery for primary species delimitation. *Molecular Ecology*, 21, 1864–1877. Available from: https://doi.org/10.1111/j.1365-294x.2011.05239.x

Ragionieri, L., Zúñiga-Reinoso, Á., Bläser, M. & Predel, R. (2023) Phylogenomics of darkling beetles (Coleoptera: Tenebrionidae) from the Atacama Desert. *PeerJ*, 11, e14848. Available from: https://doi.org/10.7717/peerj.14848

Rambaut, A. (2009) FigTree. Tree figure drawing tool. http://tree.bio.ed.ac.uk/software/figtree/

Roig-Juñent, S. & Flores, G.E. (2001) Historia biogeográfica de las áreas áridas de América del Sur austral. In: Llorente-Bousquets, J. & Morrone, J.J. (Eds.) *Introducción a la biogeografía en Latinoamérica: Teorías, conceptos, métodos y aplicaciones*. México: Las Prensas de Ciencias, Facultad de Ciencias, UNAM, pp. 1–277.

Ronquist, F., Teslenko, M., Van Der Mark, P., Ayres, D.L., Darling, A., Höhna, S. et al. (2012) MrBayes 3.2: efficient Bayesian phylogenetic inference and model choice across a large model space. *Systematic Biology*, 61, 539–542. Available from: https://doi.org/10.1093/sysbio/sys029

Seely, M.K. & Louw, G.N. (1980) First approximation of the effects of rainfall on the ecology and energetics of a Namib Desert dune ecosystem. *Journal of Arid Environments*, 3(1), 25–54. Available from: https://doi.org/10.1016/S0140-1963(18)31673-2

Struck, T.H., Feder, J.L., Bendiksby, M., Birkeland, S., Cerca, J., Gusarov, V.I. et al. (2018) Finding evolutionary processes hidden in cryptic species. *Trends in Ecology & Evolution*, 33(3), 153–163. Available from: https://doi.org/10.1016/j.tree.2017.11.007

Thompson, J.D., Higgins, D.G. & Gibson, T.J. (1994) CLUSTAL W: improving the sensitivity of progressive multiple sequence alignment through sequence weighting, position-specific gap penalties and weight matrix choice. *Nucleic Acids Research*, 22, 4673–4680. Available from: https://doi.org/10.1093/nar/22.22.4673

Tirado, C., Trujillo, D., Pizarro-Araya, J., Alfaro, F.M., González, S. & Carretero, M.A. (2018) Ecophysiological traits and activity patterns of coleopterans from Atacama Desert provide clues to the functional responses of small ectotherms to climate change. *Journal of Arid Environments*, 150, 21–27. Available from: https://doi.org/10.1016/j.jaridenv.2017.11.016

Trifinopoulos, J., Nguyen, L.T., von Haeseler, A. & Minh, B.Q. (2016) W-IQ-TREE: a fast online phylogenetic tool for maximum likelihood analysis. *Nucleic Acids Research*, 44, 232–235. Available from: https://doi.org/10.1093/nar/gkw256

Vidal, M.A., Pizarro-Araya, J., Jerez, V. & Ortiz, J.C. (2011) Daily activity and thermoregulation in predator–prey interaction during the Flowering Desert in Chile. *Journal of Arid Environments*, 75, 802–808. Available from: https://doi.org/10.1016/j.jaridenv.2011.04.012

Vidal, P. & Guerrero, M.G. (2007) *Los Tenebriónidos de Chile*, 1st edition. Chile: Ediciones Universidad Católica de Chile, pp. 1–478.

Vidiella, P.E., Armesto, J.J. & Gutiérrez, J.R. (1999) Vegetation changes and sequential flowering after rain in the southern Atacama Desert. *Journal of Arid Environments*, 43, 449–458. Available from: https://doi.org/10.1006/jare.1999.0565

Virgilio, M., Backeljau, T., Nevado, B. & De Meyer, M. (2010) Comparative performances of DNA barcoding across insect orders. *BMC Bioinformatics*, 11(1), 206. Available from: https://doi.org/10.1186/1471-2105-11-206

Xia, X. & Xie, Z. (2001) DAMBE: software package for data analysis in molecular biology and evolution. *Journal of Heredity*, 92, 371–373. Available from: https://doi.org/10.1093/jhered/92.4.371

Xia, X., Xie, Z., Salemi, M., Chen, L. & Wang, Y. (2003) An index of substitution saturation and its application. *Molecular Phylogenetics and Evolution*, 26, 1–7. Available from: https://doi.org/10.1016/S1055-7903(02)00326-3

Zhang, J., Kapli, P., Pavlidis, P. & Stamatakis, A. (2013) A general species delimitation method with applications to phylogenetic placements. *Bioinformatics*, 29, 2869–2876. Available from: https://doi.org/10.1093/bioinformatics/btt499

Zúñiga-Reinoso, Á., Mardones, D., Ritter, B., Flores, G.E., Giraldo-Mendoza, A.E. & Predel, R. (2023) Impact of geoclimatic events on the diversification of newly defined Megelenophorini (Coleoptera: Tenebrionidae) in South America. *Global and Planetary Change*, 228, 104212. Available from: https://doi.org/10.1016/j.gloplacha.2023.104212

Zúñiga-Reinoso, Á. & Méndez, M.A. (2018) Hidden and cryptic species reflect parallel and correlated evolution in the phylogeny of the genus *Callyntra* (Coleoptera: Tenebrionidae) of Central Chile. *Molecular Phylogenetics and Evolution*, 127, 405–415. Available from: https://doi.org/10.1016/j.ympev.2018.04.022

Zúñiga-Reinoso, Á., Pinto, P. & Predel, R. (2019) A new species of *Gyriosomus* Guerinmeneville (Coleoptera: Tenebrionidae) from the Chilean Atacama desert. *Annales Zoologici*, 69(1), 105–112. Available from: https://doi.org/10.3161/00034541ANZ2019.69.1.006

Zúñiga-Reinoso, Á., Ritter, B. & Predel, R. (2021) The colonization of the Puna and Atacama Biogeographic Province by sister clades of *Psectrascelis* (Coleoptera: Tenebrionidae): synchronous expansion without spatial overlap. *Journal of Biogeography*, 48(8), 1930–1940. Available from: https://doi.org/10.1111/jbi.14123

SUPPORTING INFORMATION

Additional supporting information can be found online in the Supporting Information section at the end of this article.

Table S1. Collection localities and GenBank accession numbers for the species of *Gyriosomus* used in this study. Voucher = Sample identification code. Sample ID = Species identification plus spot on the map of Figure 1. Locality = sampling location. Region = administrative region of Chile. Lat/Long = latitude and longitude in decimal degrees. Alt = altitude in meters above sea level. Year = sampling year. GB = accession number of each gene in GenBank repository.

Table S2. Detail of the primers used in this study.

Table S3. Supplementary information of the genes used in this study. N = number of sequenced specimens. Length = length of the sequences in base pairs. Model = model selected per codon (1st/2d/3d position) or per gene. All index of substitution saturation Iss were statistically different to the critical Iss (Iss.c).

Table S4. Convergence diagnostic values for MCMC runs from Mr. Mayes and BEAST speciation models comparison. minESS = minimum estimated sample size (ESS) among runs*. avgESS = average estimated sample size (ESS) among runs*. PSRF = potential scale reduction factor°. AICM = Akaike Information Criterion^.

Table S5. Summary table of the campaigns considered for this study, with the sampling year, sampling extension (degrees of southern latitude), kind of year (Niño/Niña/Normal) and intensity, perception of the specimen density in the field and observer of density in the field according with the list of the authors of this study. Very High: many specimens (n = over 15) of all species, in all localities visited, High: many specimens (n = 10–15) of several species, in almost all localities, visited, Moderate: some specimens (n = 5–10) of some species, in some localities visited, Low: few specimens (n = 3–5) of few species in particular localities, Very Low: very few specimens (n = 1–3) of one species in one or two localities. Kind of year and intensity of El Niño/La Niña phenomenon based on the Oceanic Niño Index (ONI) from NOAA (2024) El Nino Index Dashboard: NOAA Physical Sciences Laboratory. Available from: https://psl.noaa.gov/enso/dashboard.html (accessed 24 February 2025).

Table S6. Species delimitation analysis results detailed by the algorithm used (ABGD, ASAP, GMYC, sPTP with BI and ML trees, bPTP

with BI and ML trees and STACEY scenarios) and assigned to the main clade/group on the tree.

Table S7. Genetic distance based on the p-distance between the samples analysed. The main groups are highlighted following the colour code in Figure 1 and the bold boxes are the delimited species.

Table S8. Dichotomous key for the main phylogenetic groups in *Gyriosomus*.

Figure S1. Maximum likelihood phylogenetic tree for the genus *Gyriosomus*, derived from concatenated COI, 28S, CAD and Wg genes. The coloured boxes indicate the nine main clades/groups identified. Shimodaira–Hasegawa approximate likelihood ratio test (SH-aLRT)/ultrafast bootstrap (UFB) values are displayed near each node.

Video S1. Supplementary video.

How to cite this article: Anguita-Salinas, S., Guerrero, M., Diéguez, V.M., Pinto, P., Larrea-Meza, S., Jara-Flores, A. et al. (2026) How many cows are in the desert? Molecular phylogeny and species delimitation of the genus *Gyriosomus* (Coleoptera: Tenebrionidae: Pimeliinae) from the Atacama Desert. *Systematic Entomology*, 51(1), e70011. Available from: https://doi.org/10.1111/syen.70011